Radiation Physics and Chemistry xxx (xxxx) 110960

Contents lists available at ScienceDirect

Radiation Physics and Chemistry

journal homepage: www.elsevier.com/locate/radphyschem

Thermoluminescence of rose quartz from Minas Gerais, Brazil

R.T.E.K. Martins [a,g], I.A. Ferreira [a,g], A.O. Silva [a,g], M.C.S. Nunes [b,g], C. Ulsen [c], R. Künzel [d], M.M. Souza [e], M.L. Chithambo [f], E.M. Yoshimura [g], N.M. Trindade [g,*]

[a] Department of Physics, Federal Institute of São Paulo, São Paulo, SP, Brazil
[b] Graduate Program in Science and Technology of Materials, São Paulo State University, Sorocaba, SP, Brazil
[c] Polytechnic School, Technological Characterization Laboratory, University of São Paulo, São Paulo, SP, Brazil
[d] Department of Physics, Federal University of São Paulo, Diadema, SP, Brazil
[e] Department of Geography, Federal Institute of the South of Minas Gerais, Poços de Caldas, MG, Brazil
[f] Department of Physics and Electronics, Rhodes University, Grahamstown, South Africa
[g] Institute of Physics, University of São Paulo, São Paulo, SP, Brazil

ARTICLE INFO

Handling Editor: Dr. Chris Chantler

Keywords:
Rose quartz
Chemical characterization
Thermoluminescence
Kinetic parameters
Dosimetry

ABSTRACT

We report the thermoluminescence (TL) properties of rose quartz from Minas Gerais (Brazil), a translucent pink variety of quartz. Firstly, the sample shows a pure α-quartz phase, based on X-ray diffraction results. Also, the mineral shows a wide optical absorption band at about 500 nm, typical of rose quartz. In addition, X-ray fluorescence showed a high percentage of purity (99.1% of the SiO_2), and the inductively coupled plasma optical emission spectrometry (ICP-OES) recorded the presence of elements such as Al, Ca, Fe and Ti. The TL measurements were carried out using a commercial Risø TL/OSL reader, model DA-20, equipped with a built in $^{90}Sr/^{90}Y$ beta source, used to irradiate the sample to different radiation doses (0.01 – 1Gy). The glow curve, measured at a heating rate of 1 K/s, consists of a prominent peak at 355 K followed by other low intensity peaks at higher temperatures. Measurements of the main peak are reproducibility with a coefficient of variation (C.V.) of ~1.3% and a repeatability of ~1.8%. Kinetic analysis of the main peak was carried out using experimental methods comprising T_m-T_{stop} technique, the initial rise method, peak shape estimation and various computational methods (TGCD, TLanal, TLDecoxcel and GlowFit). The peak obeys first order kinetics, with activation energy of 0.86 eV, and a frequency factor of the order of 10^{11} s^{-1}. Finally, in the dose range studied, the peak shows a sublinear dose response after which supralinearity sets in.

1. Introduction

Quartz is the most common mineral in the Earth (Preusser et al., 2009; Topaksu et al., 2014). According to literature (Topaksu et al., 2014), approximately 12% of the mass of the Earth's crust is made of it. When chemically pure, quartz tends to be colorless and transparent and in some cases translucent (Jovanovski et al., 2022). The presence of impurities within its structure imparts color leading to varieties such as rose quartz, smoke, citrine or amethyst (Jovanovski et al., 2022; Lehmann and Bambauer, 1973). The cations Al^{3+} (0.51 Å), Ga^{3+} (0.62 Å), Fe^{3+} (0.64 Å), Ge^{4+} (0.53 Å), Ti^{4+} (0.64 Å) and P^{5+} (0.35 Å) are common impurities that substitute the Si^{4+} (0.42 Å) in the crystal lattice (Kibar et al., 2007). Furthermore, it is commonly found traces of a slight amount of water in types of quartz (Nur et al., 2015). The role of titanium in generating point defects of interest in irradiated pink quartz has been discussed elsewhere (Preusser et al., 2009). In addition, thermodynamic conditions can affect the type and concentration of impurities in the lattice, such as changes of pressure (P)–temperature (T) conditions or natural irradiation (Topaksu et al., 2012). Quartz has luminescent properties that may depend on its origin, formation condition, heat treatment and impurity content (Chithambo et al., 2007; El-Faramawy et al., 2022; Farouk et al., 2021; Preusser et al., 2009; Toktamiş et al., 2007). In addition, quartz, whose most common polymorph is the trigonal α-phase, is a natural mineral used in luminescence-based dosimetry (Preusser et al., 2009). Luminescence dosimetry is a type of ionizing radiation dosimetry that uses the luminescent properties of certain materials to quantify the absorbed dose of ionizing radiation, and thermoluminescence (TL) is an important technique used in dosimetry (Yukihara et al., 2022a, 2022b, 2022a).

TL is the luminescent emission of material (semiconductor or insulator), previously exposed to some source of radiation, when it is heated (Chen and McKeever, 1997). The TL experiment is an important tool to

* Corresponding author.
E-mail address: neilotrindade@usp.br (N.M. Trindade).

https://doi.org/10.1016/j.radphyschem.2023.110960
Received 26 December 2022; Received in revised form 24 March 2023; Accepted 2 April 2023
0969-806/

investigate the distribution of traps in a material (Randall and Wilkins, 1945). For dosimetry, the desirable characteristics that a TL material should present (McKeever, 1985): (i) a linear response in a certain dose range, (ii) a stable signal during time, *i.e.* no fast signal fading (spontaneous loss of signal), (iii) reproducible and repeatable TL signal, etc. Those characteristics are important because they can define what field of dosimetry (personal, environmental, spatial etc.) the material can be applied (Prabhu et al., 2021). According to the literature (Yüksel, 2018), TL characteristics in quartz mineral is throughout studied due to its abundance, the sensitivity to radiation, basic structure of the glow curve, and the simple thermal treatment procedure.

Despite the high abundance of quartz in the world, there are few in-depth studies of the thermoluminescent properties of Brazilian rose quartz. In this work, we present an investigation of the thermoluminescent response of rose quartz, also presenting a chemical and physical characterization of the natural samples. The TL response of the samples were evaluated by several analytical and computational methods to obtain the parameters of energy, frequency factor and kinetic order, being the methods: Peak Shape, Initial Rise, T_m-T_{stop}, Glowfit, TLanal, TGCD and TLDecoxcel.

2. Material and methods

2.1. Sample preparation

The sample studied (Fig. 1) consist of a rose quartz crystal collected from Northeast of Minas Gerais, Brazil. The quartz crystal was powdered in an agate mill and sieved to grain sizes smaller than 75 μm. In X-ray fluorescence (XRF), X-ray diffraction (XRD), Optical absorption (OA) measurements nonthermal treated powder samples were used. Inductively coupled plasma optical emission spectrometry (ICP-OES) was done using small samples cleaved from the original sample. Before all TL measurements, the powder was submitted to a thermal treatment at 673 K for 1 hour. In the dose-response and T_m-T_{stop} measurements, after each TL readout, and before the following irradiation, the sample was heated to 673 K (heating rate of 5 K/s) to clean the residual signal. In the fading, repeatability and reproducibility measurements, the sample was heated to 473 K (heating rate of 5nullK/s) to clean the main glow peak. In all TL measurements, samples with a mass of (25 ± 5) mg were used.

2.2. X-ray diffraction

The crystallinity of the sample was assessed using XRD measured in an EMPYREAN diffractometer (operating at 45 kV - 40 mA) with CuKα radiation (1.5405 Å). Diffractograms obtained over a Bragg angle 2θ between 10° and 50° (with a scanning increment of 0.025°) were compared with reference diffractogram PDF2 databases from the International Center for Diffraction Data (ICDD) and the Inorganic Crystal Structure Database (ICD) using the Malvern Panalytical HighScore Plus software™.

Fig. 1. Rose quartz Crystal (ruler is for scale reference; in centimeter).

2.3. Chemical composition analysis by X-ray fluorescence and inductively coupled plasma optical emission spectrometry

The major elements present in the sample were determined by XRF spectrometry using a Malvern Panalytical XRF spectrometer (model Zetium). On the other hand, trace element composition was obtained by ICP-OES using a Thermo Scientific (model iCap 6300 Duo). Preparatory to measurements, sample grains were fused with lithium tetraborate. Quantitative analysis was carried out by comparison with certified reference materials. Loss on ignition (LOI) was performed at ~1300 K for 2 hours. ICP-OES were conducted in samples prepared by microwave-assisted acid digestion for Al, Ca, Co, Fe, K, Ni, Ti and Zn dosage in a Horiba Ultima Expert.

2.4. Optical absorption

Optical absorption (OA) measurements intended to study the electronic structure of the quartz were carried on a sample using a Shimadzu UV-2600 spectrophotometer in the wavelength range 200–800 nm at a spectral resolution of 0.1 nm.

2.5. Thermoluminescence

From a TL glow curve, it is possible to obtain important information such as number of peaks, kinetic order (*b*), activation energy (*E*). To achieve that, Peak Shape (PS), Initial Rise (IR), T_m-T_{stop} and various computational methods as TGCD, TLanal, TLDecoxcel and GlowFit methods were used. TL measurements were carried out using a Risø TL/OSL DA-20 luminescence reader. Samples were irradiated *in-situ* using a built-in $^{90}Sr/^{90}Y$ beta source at a dose rate of 10nullmGy/s. The luminescence was detected by a bialkali photomultiplier tube (EMI 9235QB) through a 7.5 mm thick Hoya U-340 filter (transmission band 250–390 nm).

2.5.1. Analytical methods

To analyze the kinetic parameters of the TL glow peaks we used the method that considers the shape and geometric properties of the peak, named "Peak Shape" (Chen and McKeever, 1997; Pagonis et al., 2006). This method does not use any iterative procedure and does not require knowledge of the kinetic order (Pagonis et al., 2006), it can be used as a first analysis for isolated TL peaks. To obtain the kinetic order of the peak, the symmetry factor μ μ is used, the factor has been calculated by the following Eq. (1) (Bull, 1989):

$$\mu = \frac{T_2 - T_m}{T_2 - T_1} \tag{1}$$

where T_m is the temperature at the peak; T_1 and T_2 are the positions of the half-maximum intensity points on the low and high temperature sides of T_m respectively. According to the peak shape analyses, the trap activation energy (E_α) can be determined by Eq. (2).

$$E_\alpha = c_\alpha \left(\frac{k T_m^2}{\alpha} \right) - b_\alpha \left(2kT_m \right) \tag{2}$$

Where *k* is the Boltzmann constant, $^{c}\alpha$ and b_α are parameters that depend on symmetry factors $\tau = T_m - T_1, \delta = T_2 - T_m$ and $\omega = T_2 - T_1$ (Pagonis et al., 2006; Sunta, 2015), given by Eq. (3).

$$\begin{aligned} c_\tau &= 1.510 + 3.0\,(\mu - 0.42), \quad & b_\tau &= 1.58 + 4.2\,(\mu - 0.42) \\ c_\delta &= 0.976 + 7.3\,(\mu - 0.42), & b_\delta &= 0 \\ c_\omega &= 2.52 + 10.2\,(\mu - 0.42), & b_\omega &= 1 \end{aligned} \tag{3}$$

Also, the IR method was used to calculate *E*. This method can be applied for the first peak of the glow curve, for TL intensities (I_{TL}) smaller than 15% of the maximum intensity of the TL peak. Considering that the electron concentration in the TL trap is constant at the low-temperature part (the initial rise) of the peak. The TL emission intensity can be modeled according to Eq. (4).

$$I_{TL}(T) \propto \exp\left(-\frac{E}{kT}\right) \tag{4}$$

when applying the method, a graph is constructed that relates *ln (I)* as a function of 1/kT and *E* is obtained from the slope (Pagonis et al., 2006).

Most materials do not show a single peak or well separated peaks, because of that the T_m-T_{stop} method is useful to estimate the number of peaks, position, and an approximately kinetic order of TL glow curve. This method was first suggested by McKeever (1980). In an irradiated sample, the method consists of partially heating the sample until a determined temperature (T_{stop}), cooling until room temperature and then re-heating the sample to record all of the remaining signal. The position of the first maximum T_m is obtained. Doing this to increasing T_{stop} values and plotting a graph T_m *versus* T_{stop}, some characteristics that indicate the number of peaks and kinetic order can be observed (McKeever, 1980).

2.5.2. Computational methods

Various computational methods as Thermoluminescence analyst (TLanal), Thermoluminescence Glow Curve Deconvolution (TGCD), TLDecoxcel and GlowFit, all reported in the literature (Horowitz et al., 2022; Munoz et al., 2022), were used to estimate the kinetic parameters of the sample.

The TLanal program was introduced by (Chung et al., 2005, 2007) and develops the deconvolution of TL curves for first, second, general and mixed order kinetics in an interactive way. With this software, it is possible to obtain the kinetic parameters that best fit the internal equation to the experimental glow curve. The model used to fit TL curves for general order kinetics is the one described by May and Partridge (1964). Using TLanal, one can obtain the values of activation energy (*E*), frequency factor (*s*), re-trapping ratio and recombination coefficient (*R*) and order of kinetics (*b*) (Chung et al., 2005, 2007).

The TGCD is a package in RStudio program (Peng et al., 2016, 2021), and the expression used to best fit to the glow curve is to general order kinetics expression given by:

$$I(T) = I_m \; exp\left(\frac{E}{kT_m} - \frac{E}{kT}\right)\left[1 + \frac{b-1}{b}\frac{E}{kT_m}\left(\frac{T}{T_m}exp\left(\frac{E}{kT_m} - \frac{E}{kT}\right)F(\right.\right.$$

where *F(x)* is written as

$$F(x) = 1 - \frac{a_0 + a_1 x + x^2}{b_0 + b_1 x + x^2} \tag{6}$$

The program prompts for input values such as temperature at the peak (T_m), the maximum intensity (I_m) and the number of TL peaks. Through this program, we can obtain the values of activation energy (*E*), frequency factor (*s*) and kinetic order (*b*).

The TLDecoxcel is a program developed with the Excel Spreadsheet that allows the analysis of glow curves consisting of discrete energy peaks (general or mixed order) or continuous energy distribution peaks. In the case of the general order model, the TL intensity is given as follows (Kazakis, 2019):

$$I(T) = s_{n0}\,\exp\left(\frac{-E}{kT}\right) \times \left[1 + (b-1)\frac{s}{\beta}\int_{T_0}^{T}\exp\left(\frac{-E}{kT}\right)dT\right]^{\frac{-b}{b-1}} \tag{7}$$

Unlike the software presented above (TLanal and TGCD), in TLDecoxcel it is necessary to provide initial values of the kinetic parameters for the software to perform a fitting based on them.

The Glowfit software, proposed by (Puchalska and Bilski, 2006), adjusts a theorical curve according to the Randall-Wilkins model for first-order kinetic peaks ($b = 1$) to the experimental data. The parameters are obtained following Eq. (8) (Puchalska and Bilski, 2006).

$$I(T) = I_m\,\exp\left(\frac{E}{kT_m} - \frac{E}{kT}\right)\exp\left(\frac{E}{kT_m}\left(\alpha\left(\frac{E}{kT_m}\right) - \frac{T}{T_m}\exp\left(\frac{E}{kT_m} - \frac{E}{kT}\right)\alpha\left(\frac{E}{kT}\right)\right)\right) \tag{8}$$

in order to verify the quality of the fit, all the computational methods present the FOM (figure of merit) value, calculated according to Eq. (9) (Puchalska and Bilski, 2006).

$$FOM\,[\%] = \frac{\sum_i \left|y_i - y\left(x_i\right)\right|}{\sum_i y_i} \times 100\% \tag{9}$$

where y_i is the experimental value, and $y(x_i)$ is the value of the fitted function. A criteria to consider the results as a good fit is a FOM smaller than 2.5% (Balian and Eddy, 1977).

3. Results and discussion

3.1. X-ray diffraction

Fig. 2 shows the XRD pattern of the as received and irradiated (5 Gy, beta radiation) sample. As both samples showed (100), (101), (110) and (112) peaks at about 21°, 27°, 36° and 50°, respectively, in line with the literature (Silva et al., 2018), it was possible to verify that no structural change of the sample was caused when exposing to labo-

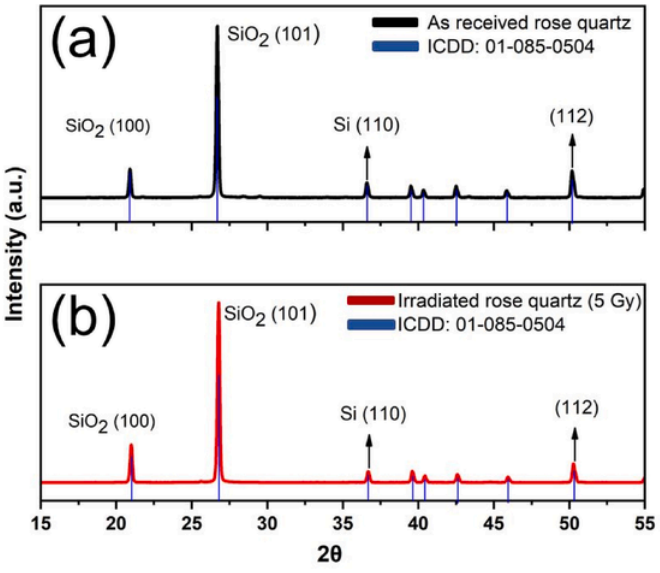

Fig. 2. X-ray diffraction (XRD) spectrum of (a) natural rose quartz for (a) non-irradiated powder sample (black diffractogram) and (b) irradiated powder sample (red diffractogram) compared with the database of the International Center for Diffraction Data (ICDD) (01-085-0504).

ratory ionizing radiation. According to database of the International Center for Diffraction Data (ICDD) (01-085-0504), the sample shows a pure α-quartz phase. In addition, from Fig. 2b it is possible to observe that no phase transition occurred because the peaks remain in the same position after irradiation and no new characteristic peak appeared.

3.2. Chemical composition analysis by X-ray fluorescence and inductively coupled plasma optical emission spectrometry

Using XRF, it was possible to identify 99.1% of the elemental composition of the SiO_2. Due to the low percentage of impurities in the rose quartz sample, as the XRF quantification results are inaccurate for elements below 1% (detection limit by XRF), ICP-OES measurement was performed to improve the characterization of the sample.

Employing ICP-OES, some impurities present in the sample were detected and are listed in Table 1. These include Al, Ca, Fe and Ti. Trace elements are present as substitutional or interstitial ions in the quartz structure. The ions that replace Si are Al, Ti, Fe, Ge, P, and Ga and interstitial ions are H, Li, Na and Fe (Preusser et al., 2009).

Table 1
– Chemical impurities of rose quartz determined by ICP-OES.

Content (mg/kg)							
Al	Ca	Co	Fe	K	Ni	Ti	Zn
254	182	<1	164	14	2	23	<1

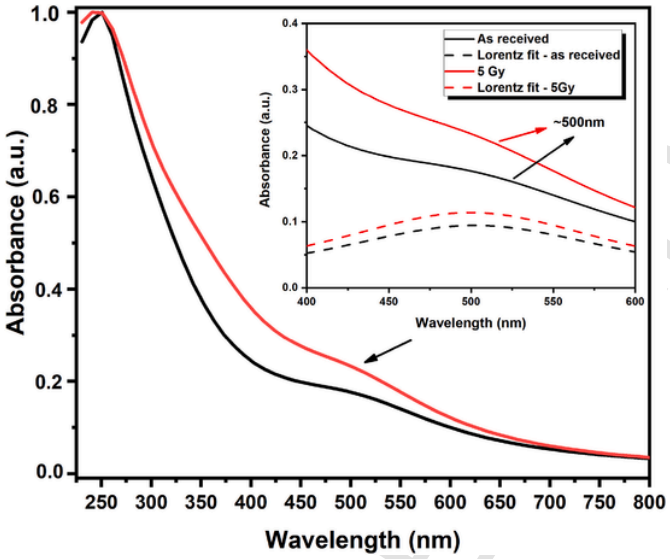

Fig. 3. Normalized optical absorption (OA) spectrum for rose quartz sample non-irradiated (black curve) and irradiated with 5 Gy (red curve). The inset is detailed between 375 and 600 nm, the dashed curves are deconvolutions using the Lorentz function.

3.3. Optical absorption

Fig. 3 shows the UV–vis absorption spectra for the rose quartz non-irradiated and irradiated (5 Gy, beta radiation) samples. The absorbance of quartz is sensitive to the origin and thermal history of the samples (Kibar et al., 2007). The quartz sample shows a broad absorbance in the UV-region and an absorbance band at about 500 nm. Results elsewhere suggest that this absorption band observed around 500 nm is responsible for the coloration of rose quartz (Götze et al., 2021; Kibar et al., 2007; Maschmeyer and Lehmann, 1983). Several studies indicate that the quartz's rose color can be assigned to nano-inclusions of dumortierite $[Al_{6.5-7}(BO_3)(SiO_4)_3(O, OH)_3]$ (Goreva et al., 2001; Götze et al., 2021; Kibar et al., 2007). Dumortierite is usually associated with quartz in hydrothermal and pegmatitic environments (Goreva et al., 2001). Fe and Ti traces are commonly detected in dumortierite samples and are associated with quartz coloration (Alexander et al., 1986). Based on the chemical analysis of our sample, in wich traces of Fe and Ti are present, we suggest that inclusion minerals such as clusters of dumortierite could be responsible for the band observed around 500 nm, assigned to the intervalence charge transfer (IVCT) between Fe^{2+} and Ti^{4+} (Kibar et al., 2007; Ma et al., 2002). The OA results show only minor changes in the optical absorption profile for the sample irradiated with a 5 Gy dose from beta radiation, indicating that the irradiation process induced no significant changes in the material.

3.4. Thermoluminescence

3.4.1. Features of the glow curve and dose response

To obtain the thermoluminescence signal from the rose quartz sample, the powdered sample was irradiated (beta doses from 0.01 to 1 Gy) and immediately readout at a heating rate of 1 K/s. Fig. 4a shows TL glow curves for different doses, being the inset the T_m position in function of dose. The same TL glow curves are plotted, in a log-log scale (Fig. 4b), for better discrimination of glow peaks. As shown in Fig. 4a it is possible to identify a main glow peak at ~355 K. From Fig. 4a inset, we concluded that the main glow peak is unchanged within the dose

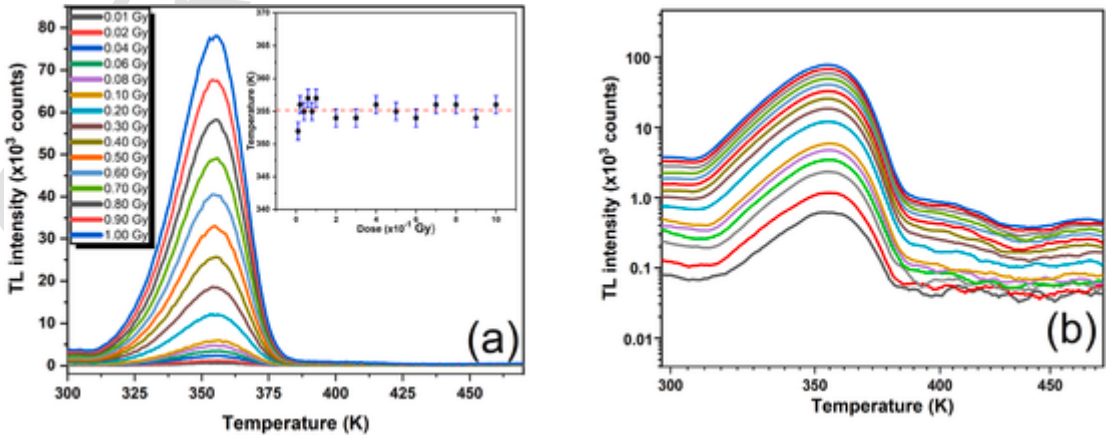

Fig. 4. (a) Glow curves of rose quartz measured at 1nullK/s following irradiation to different beta doses. The inset shows the main peak position variation with irradiation dose; the red dashed line is the peak average temperature; the blue bars are the standard deviation. (b) TL glow curves in a log-log scale. The curves have been smoothed.

range, at an average temperature of (355.3 ± 1.3) K. This indicates a first order peak, as peak position does not depend on the radiation dose. From Fig. 4b it is possible to observe two low intensity peaks at ~385 and ~420 K.

The TL glow peak of quartz at ~355 K (heating rate = 1nullK/s) occurs due to defects related to the $[AlO^4]^-$ and $[X/M^+]^+$ centers (Preusser et al., 2009). The first defect is a substitutional center produced when Al^{3+} replaces Si^{4+} in the crystal lattice of the quartz. When this occurs, the $[AlO^4]^-$ centers associate with positive charges, which can be alkaline ions (M^+), hydrogen ions (H^+), or a hole *(h)*, to compensate charge. The second defect is an interstitial ionic center, where the X defect stabilizes the alkaline interstitial ion (M^+). In this case, the X defect can be Ti or Na atoms, which, when bonding with alkaline ions (M^+), cause their stability.

Fig. 5a shows the dose-response *i.e.*, the total TL signal emitted in the temperature range studied. The inset of Fig, 5a was plotted in log-log scale to better visualize the nonlinearities, comparing to the red line (fitted for the range of 0.01–0.1 Gy) it is possible to note a nonlinearity behavior.

In general, the dose response can be described by a polynomial equation S(D) given by (Chen and McKeever, 1994; Kalita and Chithambo, 2017):

$$S(D) = k_0 + k_1 D + k_2 D^2 + k_3 D^3 + k_4 D^4 \quad (10)$$

where S(D) is the TL signal of a certain dose D; k_0, k_1, k_2, k_3 and k_4 are constants. The dose response of rose quartz could be better fitted by a 4th degree polynomial function f(D), with $R^2 = 1.0$ and residual sum of squares of ~4,4 × 10^{-7}, which the coefficients obtained were: k_0 = (15.6 ± 1.6) x10^3, k_1 = (225.8 ± 3.1) x10^4 Gy^{-1}, k_2 = (−4.1 ± 1.4) x10^5 Gy^{-2}, k_3 = (15.6 ± 2.1) x10^5 Gy^{-3}, k_4 = (−6.0 ± 1.0) x10^5 Gy^{-4}.

To characterize the dose response as supra-, sub- or linear, the superlinearity index, g(D), proposed by (Chen and McKeever, 1994), was used and it is shown in Eq. (11):

$$g(D) = \left[\frac{DS''(D)}{S'(D)}\right] + 1 \quad (11)$$

where D is the dose analyzed, S′(D) and S′′(D) is the first and second derivative of a signal S(D), g(D) is the superlinearity index, g(D) > 1 indicates a superlinear behavior; <1, sublinear; and equal to 1, linear.

The advantage of using this relation is not only because it gives the qualitative and quantitative feature of the dose response, but also because relation (11) can be applied to dose responses which the initial region is not linear, differently of the f(D) index (Chen and McKeever, 1994). Substituting Eq. (10) in Eq. (11), we get:

$$g(D) = \left[\frac{(2k_2 D + 6k_3 D^2 + 12k_4 D^3)}{(k_1 + 2k_2 D + 3k_3 D^2 + 4k_4 D^3)}\right] + 1 \quad (12)$$

Using the parameters obtained in Eq. (10) in Eq. (12), we can plot Fig. 5b, that shows the supra- sub- or linearity of dose response.

From Fig. 5b it is possible to observe a very mild sublinearity in the range from 0.01 to 0.1 Gy, after that, a supralinear increasing behavior is observed until a maximum (between 0.7 and 0.8 Gy). From 0.8 to 1 Gy there is a decrease of the supralinear behavior. Commensurate with the information of Fig. 5b, is the red line plotted in Fig. 5a: it corresponds to a linear fit (R^2 = 0.999) to the experimental points from 0.01 to 0.1 Gy.

3.4.2. Kinetic parameters from analytical methods

3.4.2.1. Main glow peak T_m-T_{stop}. Fig. 6 shows the result of the main glow peak analysis from T_m-T_{stop} method. The protocol used for the T_m-T_{stop} method was as follows.

1. Irradiation of the sample with 1 Gy;
2. heating the sample at a constant rate (β = 5 K/s) up to a T_{stop} temperature;
3. Cooling down the sample to room temperature;
4. Acquisition of a full TL glow curve, from RT to 673 K (β = 1 K/s), and determination of the temperature, T_m, of the peak.

This sequence was repeated several times, increasing T_{stop} by 3 K from 303 K up to 423 K, thus completing the whole TL curve.

In T_m-T_{stop} analysis three peaks can be observed, the peak 1 (main glow peak at ~355 K) begins in 300 K and finishes at about 375 K. A second glow peak at ~385 K and a third one at ~420 K. The peaks seen in T_m-T_{stop} analysis are consistent with those seen in Fig. 4b. At higher temperatures probably there are other peaks, nonetheless, all the low intensity peaks were not further analyzed here.

The constancy of T_m with the increase of T_{stop} is expected for a first-order kinetics TL peak, while a shift toward higher temperatures characterizes a non-first order kinetics TL peak (McKeever, 1985). Accordingly, the main glow peak (with a red line that is the average temperature T_m) presents first-order kinetics. The other glow peaks were not characterized in this work due to the low intensity in relation to the main glow peak shown by Fig. 4a.

3.4.2.2. Peak shape method and initial rise results. Based on the Peak Shape method, the value of μ = 0.42 ± 0.01 0.42 ± 0.01 was obtained for our samples (1 Gy dose and a heating rate of 1nullK/s). According to literature (Chen, 1969a), $\mu \cong\cong 0.42$ indicates a first-order peak and $\mu \cong$

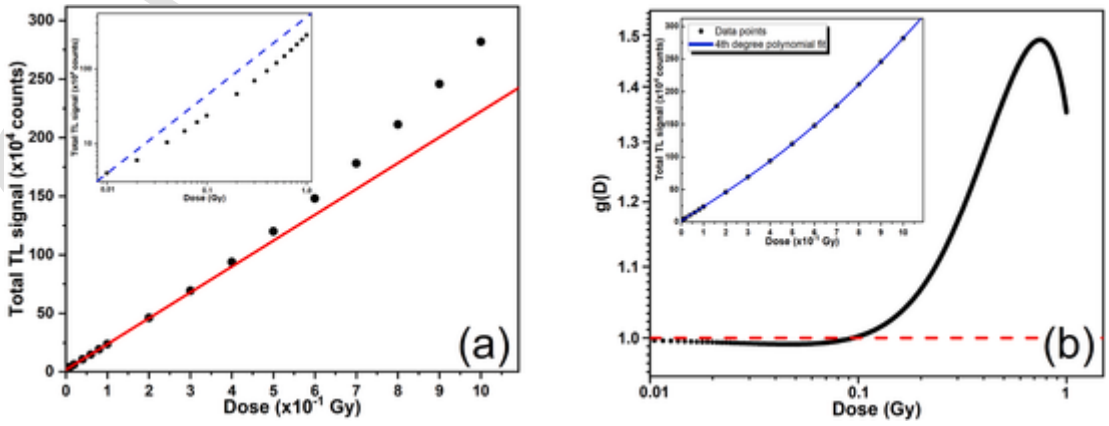

Fig. 5. (a) Dose response for the range 0.01–1 Gy; the inset is the graph plotted in a log-log scale for better visualization of the nonlinearities, the dashed blue represents the linear response. (b) The g(D) calculated for the range studied; the inset is a polynomial fit used in the region of 0.01–0.1Gy.

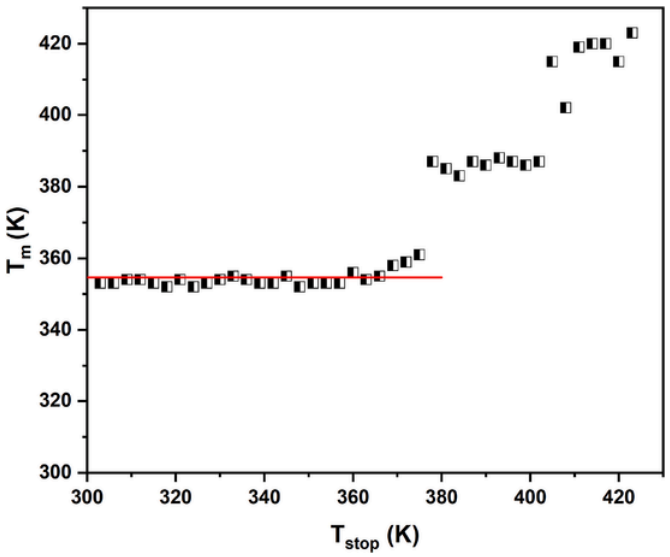

Fig. 6. T_m-T_{stop} curve from rose quartz where TL main glow peak is identified. The sample was previously irradiated with 1 Gy.

≅ 0.52 is attributed to a second-order peak. Accordingly, our analysis, indicates a first kinetics order, corresponding to $b = 1.0$ (Chen, 1969b; Sunta, 2015). Based on Eqs. (2) and (3), the results obtained for the trap activation energy for the main TL peak of rose quartz were $E_\tau = (0.86 \pm 0.04)$ eV; $E_\delta = (0.85 \pm 0.07)$ eV and $E_\omega = (0.86 \pm 0.05)$ eV.

$E_\tau = (0.86 \pm 0.04)$ eV; $E_\delta = (0.85 \pm 0.07)$ eV and $E_\omega = (0.86 \pm 0.05)$ eV.

For the Initial Rise method, the activation energy be determined using the slope of the graph shown in Fig. 7, *ln (I)* as a function of 1/kT for the initial rise of the TL glow peak recorded for rose quartz irradiated at different doses (0.02–1.0 Gy).

The average for the activation energies obtained for the best fits for the different doses was (0.82 ± 0.03) eV, a value close to that obtained by the peak shape method.

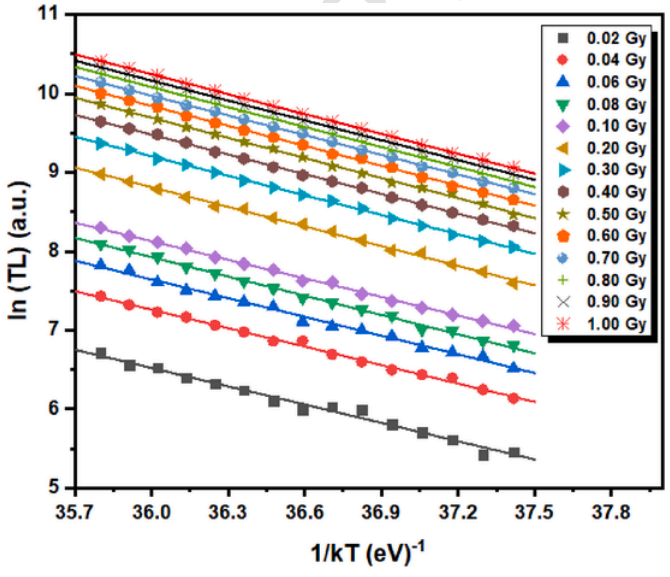

Fig. 7. Initial rise method applied on TL glow curve of the rose quartz for various doses.

3.4.3. Kinetic parameters from computational methods

3.4.3.1. TLanal. To determine the activation energy, kinetic order, and frequency factor of rose quartz glow curve, the deconvolution using single peak was done by TLanal. For this, the glow curves of doses from 0.01 to 1 Gy were obtained from heating from the room temperature up to 380 K. As shows Table 2, the average activation energy was (0.87 ± 0.01) eV, for frequency factor was obtained values that varies between 3.89 x 10^{10} 3.89×10^{10} and 2.92 x 10^{11} 2.92×10^{11} s^{-1} and the kinetic order was determined as 1.05 ± 0.01.

3.4.3.2. TGCD. For comparison purposes, the TGCD software was used to perform the deconvolution of the same TL curves data and determine the parameters of activation energy, kinetic order and frequency factor. In Table 3 the results are shown. The average of activation energy, frequency factor and kinetic order were, respectively, $E = (0.87 \pm 0.01)$ eV, $s = (1.98 \pm 0.60)$ x 10^{11} $(1.98 \pm 0.60) \times 10^{11}$ s^{-1} and $b = 1.05 \pm 0.01$.

3.4.3.3. TLDecoxcel. To deconvolve the TL curve using TLDecoxcel, it is necessary to provide initial parameters of T_m, I_m, activation energy

Table 2
–TLanal results of energy (E), frequency factor (s) and kinetic order (b) for different doses.

Dose (Gy)	b	E (eV)	s (s^{-1})	FOM
0.01	1.08	0.83	3.89 x 10^{10} $\times 10^{10}$	5.91
0.02	1.03	0.83	5.30 x 10^{10} $\times 10^{10}$	4.55
0.04	1.07	0.88	2.11 x 10^{11} $\times 10^{11}$	2.17
0.06	1.06	0.87	1.94 x 10^{11} $\times 10^{11}$	2.39
0.08	1.06	0.88	2.21 x 10^{11} $\times 10^{11}$	1.99
0.1	1.03	0.86	1.27 x 10^{11} $\times 10^{11}$	2.11
0.2	1.06	0.88	2.63 x 10^{11} $\times 10^{11}$	1.03
0.3	1.05	0.87	2.09 x 10^{11} $\times 10^{11}$	0.87
0.4	1.06	0.88	2.75 x 10^{11} $\times 10^{11}$	1.04
0.5	1.05	0.88	2.30 x 10^{11} $\times 10^{11}$	0.88
0.6	1.06	0.88	2.51 x 10^{11} $\times 10^{11}$	0.76
0.7	1.05	0.88	2.46 x 10^{11} $\times 10^{11}$	0.67
0.8	1.05	0.88	2.51 x 10^{11} $\times 10^{11}$	0.60
0.9	1.05	0.88	2.61 x 10^{11} $\times 10^{11}$	0.64
1	1.05	0.88	2.92 x 10^{11} $\times 10^{11}$	0.71
Average	1.05	0.87	2.20 x 10^{11} $\times 10^{11}$	

Table 3
–TGCD results of energy (E), frequency factor (s) and kinetic order (b) for different doses.

Dose (Gy)	b	E (eV)	s (s^{-1})	FOM
0.01	1.06	0.80	1.75 x 10^{10} $\times 10^{10}$	5.83
0.02	1.04	0.83	5.24 x 10^{10} $\times 10^{10}$	4.56
0.04	1.07	0.87	1.90 x 10^{11} $\times 10^{11}$	2.11
0.06	1.05	0.86	1.40 x 10^{11} $\times 10^{11}$	2.36
0.08	1.06	0.87	1.90 x 10^{11} $\times 10^{11}$	1.86
0.1	1.03	0.85	1.02 x 10^{11} $\times 10^{11}$	2.07
0.2	1.06	0.88	2.60 x 10^{11} $\times 10^{11}$	1.03
0.3	1.05	0.87	1.90 x 10^{11} $\times 10^{11}$	0.86
0.4	1.06	0.88	2.63 x 10^{11} $\times 10^{11}$	1.01
0.5	1.04	0.87	1.98 x 10^{11} $\times 10^{11}$	0.85
0.6	1.05	0.88	2.30 x 10^{11} $\times 10^{11}$	0.73
0.7	1.05	0.88	2.35 x 10^{11} $\times 10^{11}$	0.65
0.8	1.05	0.88	2.59 x 10^{11} $\times 10^{11}$	0.58
0.9	1.04	0.88	2.33 x 10^{11} $\times 10^{11}$	0.61
1	1.04	0.88	2.36 x 10^{11} $\times 10^{11}$	0.68
Average	1.05	0.87	1.98 x 10^{11} $\times 10^{11}$	

and kinetic order. These values are shown in Table 4 and it were estimated from the results obtained in the TGCD for each glow curve (dose range: 0.01–1 Gy). The average values of activation energy, frequency factor and kinetic order were, respectively, (0.87 ± 0.01) eV, (1.99 ± 0.61) x 10^{11} $1.99 \pm 0.61)\times10^{11}$ s^{-1} and 1.05 ± 0.01.

3.4.3.4. Glowfit. The Glowfit software was used to deconvolute the same glow curves present before. A set of initial parameters (I_m and T_m) was provided for the fitting. Only one peak was fitted for each glow curve, resulting in the average values of activation energy and frequency factor as, respectively, (0.85 ± 0.01) eV and (9.21 ± 2.27) x $10^{11}$$9.21 \pm 2.27)\times10^{11}$ s^{-1}, as Table 5 shows.

The fitted glow curves obtained directly by the computational methods TLanal, TGCD, TLDecoxcel and GlowFit are illustrated in Fig. 8 a, b, c and d, respectively, for a beta irradiation dose of 1 Gy.

3.4.4. Kinetic parameters results

Table 6 shows E values estimated by different methods with very close values resulting in an average of (0.85 ± 0.02) eV. The frequency factor (s) was estimated using the four computational methods and are included in Table 6. All the software packages achieved an excellent fitting to the experimental data (FOM <2.5%). The average value of s can be estimated approximately in the range of 1.98 x 10^{11} 1.98×10^{11} s^{-1} to 9.21 x $10^{11}$$9.21\times10^{11}$ s^{-1}, being TGCD the method that resulted in the lowest value. According to literature (Dawam and Chithambo, 2018), values of s have been reported with orders of magnitude from 10^{12} and 10^{13} s^{-1} for first-order glow peak situated in 343 K for the unannealed synthetic quartz.

In addition, the kinetic order (b) was estimated using each of the methods already described. The TL main glow peak of rose quartz follows the first-order kinetic (b = 1).

In summary, the kinetic parameters to characterize the main TL glow peak of rose quartz were determined, and they can be used to evaluate or predict features as the TL signal fading. The use deconvolution methods, requires the implementation analytical techniques to estimate the initial parameters necessary to the deconvolution, such as the number of TL glow peaks that compose the total TL curve and the peak temperatures. In addition, the determination of kinetic parameters by different methods provides an increase in the reliability of the obtained results. In our case, as there was no large variation in the parameters obtained, it can be concluded that their values were independent of the method used to obtain them.

Table 4
–TLDecoxcel results of energy (E), frequency factor (s) and kinetic order (b) for different doses.

Dose (Gy)	b	E (eV)	s (s^{-1})	FOM
0.01	1.06	0.80	1.84 x 10^{10} $\times10^{10}$	5.83
0.02	1.04	0.83	5.43 x 10^{10} $\times10^{10}$	4.57
0.04	1.07	0.87	1.92 x 10^{11} $\times10^{11}$	2.11
0.06	1.05	0.86	1.38 x 10^{11} $\times10^{11}$	2.37
0.08	1.06	0.87	1.91 x 10^{11} $\times10^{11}$	1.86
0.1	1.02	0.85	9.43 x 10^{11} $\times10^{11}$	2.07
0.2	1.06	0.88	2.64 x 10^{11} $\times10^{11}$	1.03
0.3	1.05	0.87	1.92 x 10^{11} $\times10^{11}$	0.86
0.4	1.06	0.88	2.65 x 10^{11} $\times10^{11}$	1.02
0.5	1.04	0.87	1.99 x 10^{11} $\times10^{11}$	0.85
0.6	1.05	0.88	2.33 x 10^{11} $\times10^{11}$	0.74
0.7	1.05	0.88	2.39 x 10^{11} $\times10^{11}$	0.65
0.8	1.05	0.88	2.53 x 10^{11} $\times10^{11}$	0.58
0.9	1.04	0.88	2.36 x 10^{11} $\times10^{11}$	0.61
1	1.04	0.88	2.38 x 10^{11} $\times10^{11}$	0.68
Average	1.05	0.87	1.99 x 10 ^{11}1.99×10^{11}	

Table 5
–Glowfit results of energy (E), frequency factor (s) and kinetic order (b) for different doses.

Dose (Gy)	b	E (eV)	s (s^{-1})	FOM
0.01	1	0.79	1.24 x 10^{11} $\times10^{11}$	5.83
0.02	1	0.82	3.58 x 10^{11} $\times10^{11}$	4.50
0.04	1	0.84	7.17 x 10^{11} $\times10^{11}$	2.33
0.06	1	0.84	7.04 x 10^{11} $\times10^{11}$	2.49
0.08	1	0.85	8.13 x 10^{11} $\times10^{11}$	2.16
0.1	1	0.85	7.53 x 10^{11} $\times10^{11}$	2.10
0.2	1	0.85	9.42 x 10^{11} $\times10^{11}$	1.47
0.3	1	0.85	9.17 x 10^{11} $\times10^{11}$	1.17
0.4	1	0.85	1.05 x 10^{12} $\times10^{12}$	1.47
0.5	1	0.85	9.97 x 10^{11} $\times10^{11}$	1.21
0.6	1	0.85	1.02 x 10^{12} $\times10^{12}$	1.19
0.7	1	0.85	1.06 x 10^{12} $\times10^{12}$	1.12
0.8	1	0.86	1.13 x 10^{12} $\times10^{12}$	1.06
0.9	1	0.86	1.18 x 10^{12} $\times10^{12}$	1.01
1	1	0.86	1.26 x 10^{12} $\times10^{12}$	1.10
Average	1	0.85	9.21 x 10^{11} $\times10^{11}$	

3.5. Reproducibility and repeatability

An important desirable property in thermoluminescence materials dosimetry is the signal reproducibility and repeatability. To verify if a material is reproducible and repeatable the coefficient of variation (C.V. = standard deviation/average) is used. In this study C. V. was calculated for repetitions with 10 samples or 10 readouts of the same sample. The results are presented in Fig. 9, giving rise to a C.V. of 1.3% for reproducibility and 1.8% for repeatability. It is expected that reproducible/repeatable TL system demonstrates a C.V. smaller than 5% (Furetta, 2003).

3.6. Fading and lifetime

Other important characteristic of a material is the capability of keeping the signal during storage time. A way to understand how the spontaneous escape of trapped electrons work in a material is to perform a fading test, that is, the sample is irradiated with a different delays before the TL measurement.

Using the intensity values normalized by the corresponding value obtained immediately after a 1 Gy irradiation, the reduction of the TL signal (fading) of the sample was investigated for different storage times. The results are presented in Fig. 10 where it is show for 1h delay, the sample showed an almost total loss of signal, remaining only ~12%. The deconvolution of the glow curves related to this fading experiment were done using TGCD package to verify if there were changes in the kinetic parameters. The results are presented in Table 7.

The results for E varied between 0.89 and 0.96 eV, while for the values of b we obtained between 1.04 and 1.09, *i.e.,* first order kinetics. The highest calculated activation energy was obtained for the 3600nulls (1h) storage time, in which the main TL peak fades ~90% of its total signal. Possibly, the variation in activation energy for longer storage times is due to the influence of the second TL peak, making it necessary to include a second peak in the deconvolution.

Based in the activation energy (E) and the frequency factor (s) through the different methods, it is possible to the estimate the lifetime (τ) of a TL peak (Eq. (13)) when kept at a fixed temperature (T = 295 K). The calculated lifetime can be compared to fading test to verify if the mathematical approach is right.

$$\tau = s^{-1} \exp\left(\frac{E}{kT}\right) \quad (13)$$

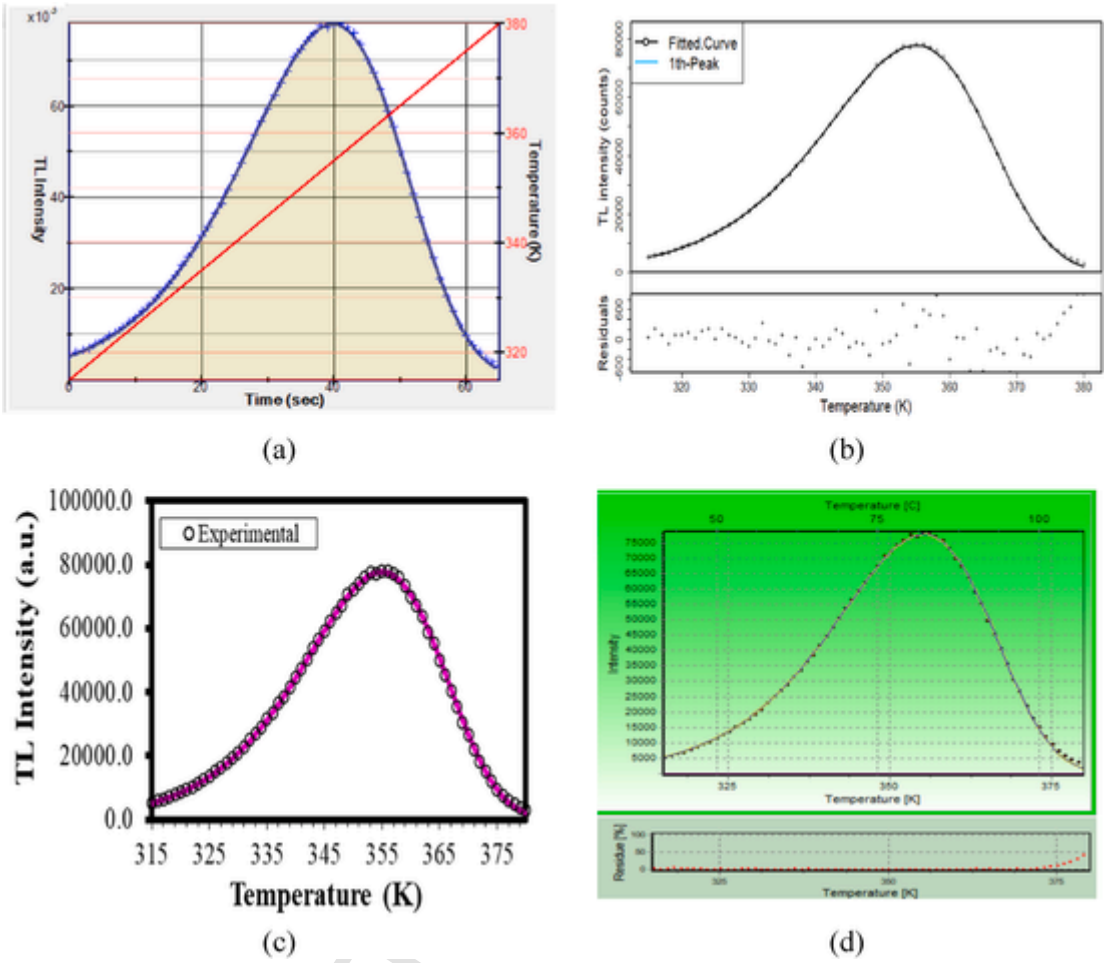

Fig. 8. Deconvolution applied to the glow curve of the sample irradiated with 1 Gy of beta radiation by (a) TLanal, (b) TGCD, (c) TLDecoxcel, and (d) Glowfit. In (a), the red line corresponds to the temporal evolution of the temperature. In (b) and (d) the residues are shown at the bottom.

Table 6
– Peak Shape and computational methods results of energy (E), frequency factor (s) and kinetic order (b).

Methods	E (eV)	s (x$10^{11}s^{-1}$)	b
Chen's τ	0.86 ± 0.04	–	1[a]
Chen's δ	0.85 ± 0.05	–	–
Chen's ω	0.86 ± 0.07	–	–
Initial Rise	0.82 ± 0.02	–	–
TLanal	0.87 ± 0.01	2.20	1.05 ± 0.01
TGCD	0.87 ± 0.01	1.98	1.05 ± 0.01
TLDecoxcel	0.87 ± 0.01	1.99	1.05 ± 0.01
GlowFit	0.85 ± 0.01	9.21	1[b]

[a] Determined by the geometric factor (μ).
[b] GlowFit analysis software is based on the first-order kinetics mode.

It was considered the average of all methods used in this work, $s = 1.67 \times 10^{11} s^{-1}$, $E = 0.87$ eV and $T = 295$ K, to calculate the lifetime (τ). It resulted approximately ~1 hour, agreeing with fading results.

4. Conclusion

In the present paper, a rose quartz sample from Minas Gerais (Brazil) and its thermoluminescence properties were analyzed. In the XRD results it was verified that the sample consists of a α-quartz crystalline phase. The chemical characterization confirmed a 99.1% of Silica (SiO_2) content by XRF, and trace elements such as Al, Ca and Fe by ICP-OES. TL analyses showed that the sample presents an intense glow peak in ~355 K, at a heating rate of 1nullK/s. The TL dose response showed a weak sublinear behavior in the dose range from 0.01 to 0.1 Gy and, after that, a supralinear tendency. The kinetic parameters obtained using many software analyses. The computational results demonstrated the quartz TL peak is first-order kinetics ($b = 1$), with activation energy (E) of ~0.86 eV and frequency factor (s) of ~ 3.62 x 10^{11} $3.62 \times 10^{11} s^{-1}$. The sample signal proved to be repeatable for a same sample with a C.V. of ~1.80% and for reproducible, with a C.V. of ~1.30% with 10 samples. Finally, the sample showed a fast fading, remaining 12% of the total signal with a lifetime of approximately 1 hour, that was confirmed with a lifetime calculation with the parameters E and s.

The use of natural materials as detection and measurement of ionizing radiation has the advantage of availability and low manufacturing cost compared to synthetic materials. With this work we expect to have contributed with useful information regarding the use of rose quartz luminescence properties for dosimetry purposes.

Author statement

R. T. E. K. Martins: Methodology, Formal analysis, Investigation, Data Curation, Writing - Original Draft, Visualization. I. A. Ferreira: Methodology, Formal analysis, Investigation, Data Curation, Writing - Original Draft, Visualization. A. O. Silva: Methodology, Formal analysis, Investigation, Data Curation, Writing - Original Draft, Visualization. M. C. S. Nunes: Methodology, Formal analysis, Investigation, Data Curation, Writing - Original Draft, Visualization. C. Ulsen: Resources,

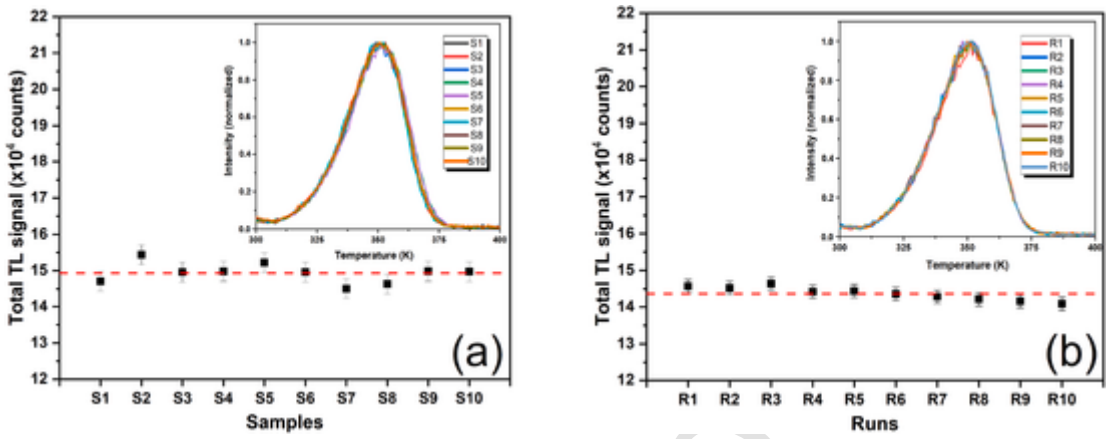

Fig. 9. (a) Reproducibility from 10 different samples of the same mass. (b) Repeatability from 10 different readout of the same sample. The inset is the normalized TL glow curves. The samples were previously irradiated with 1 Gy.

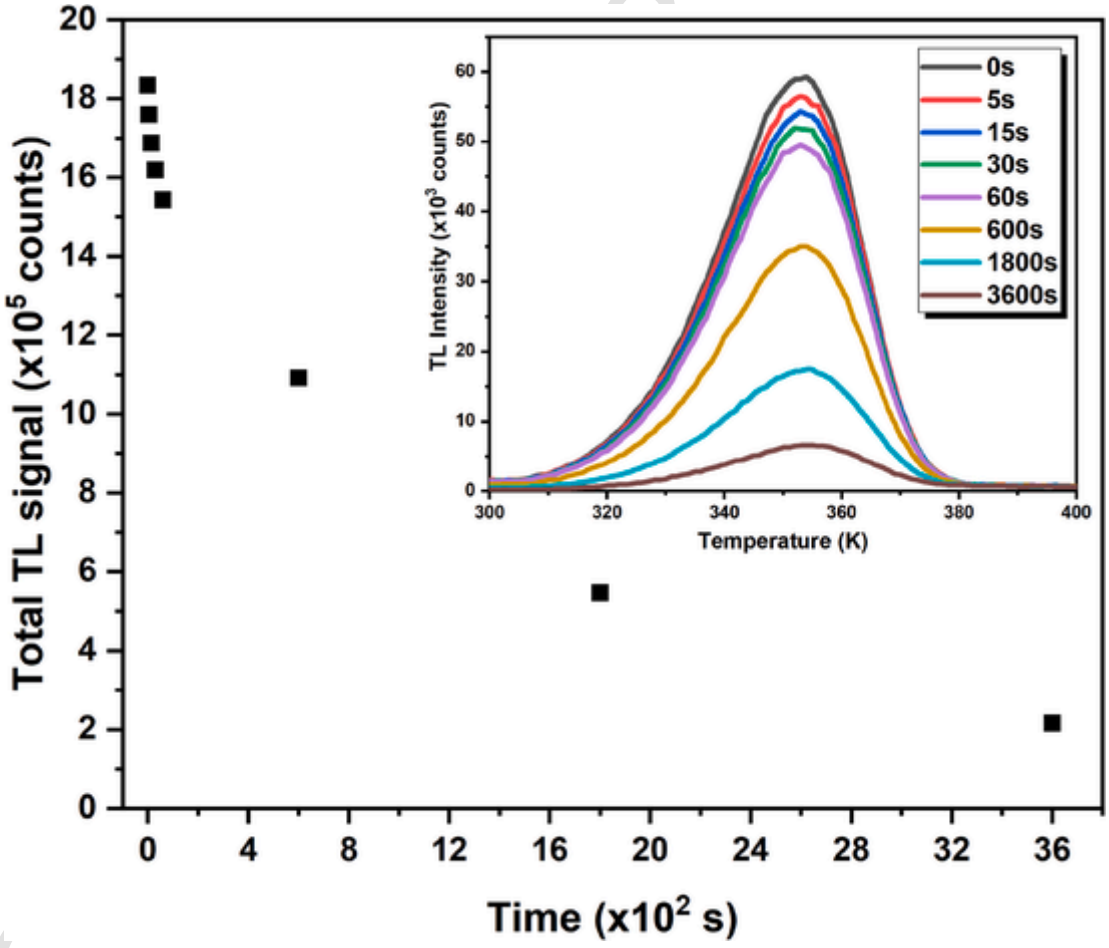

Fig. 10. Total TL intensity (area) of the rose quartz sample glow curves as a function of the storage time. The inset presents glow curve obtained for different storage times. The sample was previously irradiated with 1 Gy.

Writing-Review&Editing. R. Kunzel: Data Curation, Resources, Writing - Original Draft, Writing-Review&Editing. M. M. Souza: Resources, Writing - Original Draft. M. L. Chithambo: Methodology, Writing-Review&Editing. E. M. Yoshimura: Resources, Validation, Writing-Review&Editing. N. M. Trindade: Conceptualization, Methodology, Validation, Writing - Original Draft, Writing-Review&Editing, Funding acquisition.

Declaration of competing interest

The authors declare that they have no known competing financial interests or personal relationships that could have appeared to influence the work reported in this paper.

Data availability

Data will be made available on request.

Table 7
–TGCD results of energy (E) and kinetic order (b) for different storage times.

Storage time (s)	E (eV)	b
0	0.90	1.04
5	0.89	1.04
15	0.89	1.04
30	0.90	1.04
60	0.90	1.05
600	0.90	1.06
1800	0.91	1.09
3600	0.96	1.09

Acknowledgements

R.T.E.K. Martins thanks to PIBIC (#2021/SPO.0103) and FAPESP (#2022/07200–4). I.A. Ferreira thanks to FAPESP (#2021/05042–0). A.O. Silva thanks to FAPESP (#2020/15626–6). M.C.S. Nunes thanks to FAPESP (#2021/12758–1). R. Künzel thanks to FAPESP (#2021/10117-9). M.M. Souza thanks the research support from the IFSP/IFSULDEMINAS. E.M. Yoshimura is grateful to FAPESP (#2018/05982–0) and CNPq (#311657/2021–4). N.M. Trindade thanks FAPESP (#2018/05982–0; #2019/05915–3) and CNPq (#409338/2021–4).

References

Alexander, V.D., Griffen, D.T., Martin, T.J., 1986. Crystal chemistry of some Fe- and Ti-poor dumortierites. Am. Mineral. 71, 786–794.
Balian, H.G., Eddy, N.W., 1977. Figure-of-merit (FOM), an improved criterion over the normalized chi-squared test for assessing goodness-of-fit of gamma-ray spectral peaks. Nucl. Instrum. Methods 145, 389–395. https://doi.org/10.1016/0029–554X(77)90437-2.
Bull, R.K., 1989. Kinetics of the localised transition model for thermoluminescence. J. Phys. D Appl. Phys. 22, 1375–1379. https://doi.org/10.1088/0022-3727/22/9/022.
Chen, R., 1969a. Glow curves with general order kinetics. J. Electrochem. Soc. 116, 1254. https://doi.org/10.1149/1.2412291.
Chen, R., 1969b. On the calculation of activation energies and frequency factors from glow curves. J. Appl. Phys. 40, 570–585. https://doi.org/10.1063/1.1657437.
Chen, R., McKeever, S.W.S., 1997. Theory of Thermoluminescence and Related Phenomena. World Scientific Publishing Co. https://doi.org/10.1142/2781.
Chen, R., McKeever, S.W.S., 1994. Characterization of nonlinearities in the dose dependence of thermoluminescence. Radiat. Meas. 23, 667–673. https://doi.org/10.1016/1350-4487(94)90002-7.
Chithambo, M.L., Preusser, F., Ramseyer, K., Ogundare, F.O., 2007. Time-resolved luminescence of low sensitivity quartz from crystalline rocks. Radiat. Meas. 42, 205–212. https://doi.org/10.1016/J.RADMEAS.2006.07.005.
Chung, K.S., Choe, H.S., Lee, J.I., Kim, J.L., 2007. A new method for the numerical analysis of thermoluminescence glow curve. Radiat. Meas. 42, 731–734. https://doi.org/10.1016/j.radmeas.2007.02.028.
Chung, K.S., Choe, H.S., Lee, J.I., Kim, J.L., Chang, S.Y., 2005. A computer program for the deconvolution of thermoluminescence glow curves. Radiat. Protect. Dosim. 115, 343–349. https://doi.org/10.1093/rpd/nci073.
Dawam, R.R., Chithambo, M.L., 2018. Thermoluminescence of annealed synthetic quartz: the influence of annealing on kinetic parameters and thermal quenching. Radiat. Meas. 120, 47–52. https://doi.org/10.1016/J.RADMEAS.2018.06.004.
El-Faramawy, N., Alazab, H.A., Gad, A., Sabry, M., 2022. Study of the thermoluminescence kinetic parameters of a β-irradiated natural calcite. Radiat. Phys. Chem. 190, 109793. https://doi.org/10.1016/j.radphyschem.2021.109793.
Farouk, S., Gad, A., Al-Azab, H., El-Nashar, H., El-Faramawy, N., 2021. Thermoluminescence response and its kinetic analysis of a natural milky quartz associated with tin-tungsten-fluorite mineralization. Radiat. Phys. Chem. 181, 109333. https://doi.org/10.1016/j.radphyschem.2020.109333.
Furetta, C., 2003. Handbook of Thermoluminescence, Handbook of Thermoluminescence. World Scientific Publishing Co. https://doi.org/10.1142/5167.
Goreva, J.S., Ma, C., Rossman, G.R., 2001. Fibrous nanoinclusions in massive rose quartz: the origin of rose coloration. Am. Mineral. 86, 466–472. https://doi.org/10.2138/AM-2001-0410.
Götze, J., Pan, Y., Müller, A., 2021. Mineralogy and mineral chemistry of quartz: a review. Mineral. Mag. 85, 639–664. https://doi.org/10.1180/mgm.2021.72.
Horowitz, Y.S., Oster, L., Reshes, G., Nemirovsky, D., Ginzburg, D., Biderman, S., Bokobza, Y., Sterenberg, M., Eliyahu, I., 2022. Recent developments in computerised analysis of thermoluminescence glow curves: software codes, mechanisms and dosimetric applications. Radiat. Protect. Dosim. 198, 821–842. https://doi.org/10.1093/rpd/ncac147.
Jovanovski, G., Šijakova-Ivanova, T., Boev, I., Boev, B., Makreski, P., 2022. Intriguing minerals: quartz and its polymorphic modifications. ChemTexts 8, 14. https://doi.org/10.1007/s40828-022-00165-2.
Kalita, J.M., Chithambo, M.L., 2017. The influence of dose on the kinetic parameters and dosimetric features of the main thermoluminescence glow peak in α-Al_2O_3:C,Mg. Nucl. Instrum. Methods Phys. Res. Sect. B Beam Interact. Mater. Atoms 394, 12–19. https://doi.org/10.1016/j.nimb.2016.12.027.
Kazakis, N.A., 2019. TLDECOXCEL: a dynamic excel spreadsheet for the computerised curve deconvolution of tl glow curves into discrete-energy and/or continuous-energy-distribution peaks. Radiat. Protect. Dosim. 187, 154–163. https://doi.org/10.1093/rpd/ncz150.
Kibar, R., Garcia-Guinea, J., Çetin, A., Selvi, S., Karal, T., Can, N., 2007. Luminescent, optical and color properties of natural rose quartz. Radiat. Meas. 42, 1610–1617. https://doi.org/10.1016/j.radmeas.2007.08.007.
Lehmann, G., Bambauer, H.U., 1973. Quartz crystals and their colors. Angew Chem. Int. Ed. Engl. 12, 283–291. https://doi.org/10.1002/anie.197302831.
Ma, C., Goreva, J.S., Rossman, G.R., 2002. Fibrous nanoinclusions in massive rose quartz: HRTEM and AEM investigations. Am. Mineral. 87, 269–276. https://doi.org/10.2138/am-2002-2-308.
Maschmeyer, D., Lehmann, G., 1983. New hole centers in natural quartz. Phys. Chem. Miner. 10, 84–88. https://doi.org/10.1007/BF00309589.
May, C.E., Partridge, J.A., 1964. Thermoluminescent kinetics of alpha-irradiated alkali halides. J. Chem. Phys. 40, 1401–1409. https://doi.org/10.1063/1.1725324.
McKeever, S.W.S., 1985. Thermoluminescence of Solids, Thermoluminescence of Solids. Cambridge University Press. https://doi.org/10.1017/cbo9780511564994.
McKeever, S.W.S., 1980. On the analysis of complex thermoluminescence. Glow-curves: resolution into individual peaks. Phys. Status Solidi 62, 331–340. https://doi.org/10.1002/pssa.2210620139.
Munoz, J.M., Yoshimura, E.M., Chithambo, M.L., Jacobsohn, L.G., Trindade, N.M., 2022. The kinetic parameters of the main thermoluminescence glow peak of Al_2O_3:C,Mg: a critical evaluation of different analytical methods. J. Lumin. 247, 118848. https://doi.org/10.1016/j.jlumin.2022.118848.
Nur, N., Yeğingil, Z., Topaksu, M., Kurt, K., Doğan, T., Sarıgül, N., Yüksel, M., Altunal, V., Özdemir, A., Güçkan, V., Günay, I., 2015. Study of thermoluminescence response of purple to violet amethyst quartz from Balikesir, Turkey. Nucl. Instrum. Methods Phys. Res. Sect. B Beam Interact. Mater. Atoms 358, 6–15. https://doi.org/10.1016/j.nimb.2015.05.011.
Pagonis, V., Kitis, G., Furetta, C., 2006. Numerical and Practical Exercises in Thermoluminescence, first ed. Springer New York, New York, NY. https://doi.org/10.1007/0-387-30090-2.
Peng, J., Dong, Z., Han, F., 2016. tgcd: an R package for analyzing thermoluminescence glow curves. SoftwareX 5, 112–120. https://doi.org/10.1016/j.softx.2016.06.001.
Peng, J., Kitis, G., Sadek, A.M., Karsu Asal, E.C., Li, Z., 2021. Thermoluminescence glow-curve deconvolution using analytical expressions: a unified presentation. Appl. Radiat. Isot. 168, 109440. https://doi.org/10.1016/j.apradiso.2020.109440.
Prabhu, N.S., Sharmila, K., Somashekarappa, H.M., Al-Ghamdi, H., Almuqrin, A.H., Sayyed, M.I., Kamath, S.D., 2021. Enhanced thermoluminescence intensity, stability, and sensitivity of the Yb^{3+} doped BaO–ZnO–LiF–B_2O_3 glass by Sm^{3+} co-doping. Mater. Chem. Phys. 271, 124906. https://doi.org/10.1016/j.matchemphys.2021.124906.
Preusser, F., Chithambo, M.L., Götte, T., Martini, M., Ramseyer, K., Sendezera, E.J., Susino, G.J., Wintle, A.G., 2009. Quartz as a natural luminescence dosimeter. Earth Sci. Rev. 97, 184–214. https://doi.org/10.1016/j.earscirev.2009.09.006.
Puchalska, M., Bilski, P., 2006. GlowFit—a new tool for thermoluminescence glow-curve deconvolution. Radiat. Meas. 41, 659–664. https://doi.org/10.1016/j.radmeas.2006.03.008.
Randall, J.T., Wilkins, M.H.F., 1945. Phosphorescence and electron traps - I. The study of trap distributions. Proc. R. Soc. London. Ser. A. Math. Phys. Sci. 184, 365–389. https://doi.org/10.1098/rspa.1945.0024.
Silva, C.M., Rosseel, T.M., Kirkegaard, M.C., 2018. Radiation-induced changes in quartz, A mineral analog of nuclear power plant concrete aggregates. Inorg. Chem. 57, 3329–3338. https://doi.org/10.1021/acs.inorgchem.8b00096.
Sunta, C.M., 2015. Unraveling Thermoluminescence. In: Springer Series in Materials Science Springer Series in Materials Science. Springer India, New Delhi. https://doi.org/10.1007/978-81-322-1940-8.
Toktamiş, H., Yazici, A.N., Topaksu, M., 2007. Investigation of the stability of the radiation sensitivity of TL peaks of quartz extracted from tiles. Nucl. Instrum. Methods Phys. Res. Sect. B Beam Interact. Mater. Atoms 262, 69–74. https://doi.org/10.1016/j.nimb.2007.05.003.
Topaksu, M., Correcher, V., Garcia-Guinea, J., Topak, Y., Göksu, H.Y., 2012. Comparison of thermoluminescence (TL) and cathodoluminescence (ESEM-CL) properties between hydrothermal and metamorphic quartzes. Appl. Radiat. Isot. 70, 946–951. https://doi.org/10.1016/j.apradiso.2012.03.017.
Topaksu, M., Dogan, T., Yüksel, M., Kurt, K., Topak, Y., Yegingil, Z., 2014. Comparative study of the thermoluminescence properties of natural metamorphic quartz belonging to Turkey and Spain. Radiat. Phys. Chem. 96, 223–228. https://doi.org/10.1016/j.radphyschem.2013.10.014.
Yukihara, E.G., Bos, A.J.J., Bilski, P., McKeever, S.W.S., 2022a. The quest for new thermoluminescence and optically stimulated luminescence materials: needs, strategies and pitfalls. Radiat. Meas. 158, 106846. https://doi.org/10.1016/j.radmeas.2022.106846.
Yukihara, E.G., McKeever, S.W.S., Andersen, C.E., Bos, A.J.J., Bailiff, I.K., Yoshimura, E.M., Sawakuchi, G.O., Bossin, L., Christensen, J.B., 2022b. Luminescence dosimetry. Nat. Rev. Methods Prim. 2, 26. https://doi.org/10.1038/s43586-022-00102-0.
Yüksel, M., 2018. Thermoluminescence and dosimetric characteristics study of quartz samples from Seyhan Dam Lake Terraces. Can. J. Phys. 96, 779–783. https://doi.org/10.1139/cjp-2017-0741.